Direct Measurements of Reynolds Stresses and Turbulence in the Bottom Boundary Layer

Joseph Katz
Department of Mechanical Engineering, and
Center for Environmental and Applied Fluid Mechanics
Johns Hopkins University, 3400 N. Charles Street
Baltimore, MD 21218
phone: (410) 516-5470 fax: (410) 516-7254 email: katz@titan.me.jhu.edu

Thomas Osborn
Department of Earth and Planetary Sciences, and
Center for Environmental and Applied Fluid Mechanics
The Johns Hopkins University
3400 N Charles Street
Baltimore, MD 21218-2681
phone (410) 516-7039 fax (410) 516-7933 email osborn@jhu.edu

Award Number: N000149510215

LONG-TERM GOALS

a. Measure the Reynolds stresses, velocity profile, vorticity distribution and transport, dissipation rate, and turbulent spectra (energy and dissiaption) in the bottom boundary layer of the coastal ocean using Particle Image Velocimetry (PIV). The objective is to obtain data that is free of wave contamination.

b. Quantify the temporal variation of turbulent stresses, turbulence production, dissipation and spectra in relation to the oceanographic parameters that represent the local environment, such as waves, currents, vertical density gradient, internal waves and nature of the water-sediment interface. The conclusions will quantify the relative importance of different mechanisms that control the flow and turbulence in the benthic boundary layer.

c. Study the mechanisms and extent of sediment re-suspension process, while measuring the details of the evolving flow structure causing this entrainment. The data will enable us to determine whether sediment re-suspension is caused by large scale eddies, as small scale laboratory studies and atmospheric boundary layer data seem to indicate, shear caused by the mean flow over the bottom, or interaction of mean flow with ripples or other bottom features.

d. Use oceanic PIV data for Addressing Sub-Grid Scale Modeling issues for Large Eddy Simulation.

e. The availability of 2-D instantaneous velocity distributions enables us to examine the structure of the flow and study the vertical vorticity transport as well as formation of large coherent vortex structures near the bottom and their migrations upward. Included are, for e.g., ejections, hair-pin vortices and internal shear layers. Presently there is very little information on the dynamics and impact of large coherent structure in bottom boundary layer. Sediment entrainment is a phenomena that is closely associated with large coherent vortex structures.

OBJECTIVES

Our effort for the past year focused on several objectives:

a. Continuation and completion of the analysis of PIV data that had obtained in previous deployments. In particular the effort focused on existence of anisotropy at small scales.

b. Assemble and deploy an enhanced PIV system that will enable us to measure special turbulent spectra and Reynolds stresses without wave "contamination". Details of a recent successful deployment of this system are described in the following sections.

APPROACH

Particle image velocimetry (PIV) is capable of mapping two components of the instantaneous velocity distribution within an entire section of a flow field. This method consists of illuminating selected sections of the flow field with a laser sheet. If the laser is pulsed more than once while recording a single (or two) image(s), each particle within the sample plane leaves multiple traces on the same (or successive) recording medium (media). Data analysis consists of dividing the image into a large number of small windows and computing the mean displacement of all the particles within each window. Typically, the analysis is based on computing the auto-correlation function of the intensity distribution within the selected window. In ocean applications natural seeding is sufficient for obtaining high quality data. As described below, this year we have successfully deployed an advanced PIV system with multiple laser sheets and massive image acquisition system.

WORK COMPLETED

The original submersible PIV system with 20x20 cm^2 sample area (see Bertuccioli et al., 1999 for a detailed description of this system) was deployed in the New York Bight, 7 miles east of Sandy Hook, NJ, in June 1998. The measurements were performed at six different elevations ranging from 10 cm to about 1.4 m above the sea floor. The data for each elevation consists of 130 image pairs recorded at 1 Hz. With an image size of 1024 x 1024 pixels, an interrogation window size of 64 x 64 pixels and 50% overlap between adjacent windows, each image pair produces a map of 29 x 29 instantaneous velocity vectors. Thus, data processing provides a series of 130 two dimensional, instantaneous velocity distributions within the sample area. Subsequent analysis that has continued until this year provides distributions of mean velocity and spatial spectra of energy and dissipation rate. The data has also been used for evaluating and comparing different methods for measuring/estimating dissipation rates. Sample results are presented in the next section and further details can be found in Doron et al., (2000).

Based on the experience gained with the original oceanic PIV system, especially the effect of wave contamination on the extended-interpolated, Taylor's Hypothesis based approach, we developed, constructed and deployed a new, substantially enhanced PIV system. The new system can acquire data with resolution, size of sample area and acquisition time that address the limitations of the original setup. Several features are particularly important:

a. Continuous data acquisition is now possible, enabling us to obtain statistically converged estimates of mean flow and turbulence parameters (e.g. mean velocity and rms values of velocity fluctuations). At least 15 minutes of data at each elevation is a bare minimum.

b. The sample area has been increased to a degree that enables computations of true spatial spectra that covers the range contaminated by the surface waves. A wavenumber of 4.2 rad/m, i.e. a wavelength of 1.5 m, has been identified as an initial objective. The increased sample area does not cause a reduced resolution in the high wavenumber range.

c. With two cameras operating simultaneously the new system enables us to record data in two different planes simultaneously in order to obtain data on all the three velocity components. When one of the light sheets is vertical and aligned with the flow direction, the second sheet can be horizontal, for example, and provide data on the cross-stream velocity component. As an alternative, focusing two cameras on the same light sheet at different angles, i.e. using stereo-photography, can provides data on the three dimensional velocity distribution within the sample area.

d. The dynamic range and sensitivity of the camera as well as the quality of the submerged probes that convert the light transmitted through the fiber to a laser sheet have been substantially improved.

All of these features have been incorporated into the new PIV system that we have recently deployed near LEO-15. Schematic descriptions of the experimental setup (as it was deployed) are presented in Figures 1 and 2. The system enables us to simultaneously operate two 2048x2048 pixels^2, 4 frames/s, 12 bit digital cameras with hardware-based image shifters to overcome directional ambiguity. When these cameras record double-exposure images the two overlapping frames are shifted on the CCD array relative to each other by a prescribed number of pixels. The magnitude (in pixels) of the shift can be adjusted using the computer controlling the camera to be larger than all possible displacements in a certain direction. Consequently, all the particle traces appear to be moving in the same direction and the known fixed displacement is subtracted after processing the images. Due to the increased resolution and sensitivity of these cameras, it is possible to increase the sample size to 0.5x0.5 m^2 without compromising the smallest scales (0.6-0.8 cm) that has been used with the older setup. Each camera feeds data to a high-speed disk array with a capacity of 240 GB (six disks, 40 GB each) that can acquire data at a sustained maximum acquisition speed of 60 MB/s (only 32 MB/s are needed for the present system). When the experiment is completed the data is compressed without loss of resolution and then backed-up on another hard disk. The storage capacity of this system enables us to continuously acquire 16 bit images at 0.5 Hz for more than 15 hours (a maximum of 13 hours was actually recorded), i.e. we can cover an entire tidal cycle.

The light source of the new system is the original dual head flashlamp-pumped dye laser. It can generate 15 pulse pairs/s with essentially unlimited in-pair delay. The energy output, 350 millijoule/pulse, is sufficient for pumping light through more than one fiber. Consequently, as Figure 2 shows, in the new system we split the laser beams and focus them onto two optical fibers that transmit the light to the submerged probes. Each probe transmits about 120 mj/pulse. This setup enables us to orient the two cameras and laser sheets independently. Since the mounting rails are modular and can be easily reconfigured, we have substantial flexibility in arranging the two cameras in other configurations. For example, the two cameras can be aligned vertically in the same plane and provide data on a 1 m high strip of ocean flow. They can also be positioned in perpendicular planes and provide statistics on all the three velocity components. Stereo-photography to obtain the 3-D velocity distribution in the (single) sample area is also an option, but it would require some modifications to the orientation of the lenses relative to the CCD arrays.

Figure 1 shows the setup used during most of the recent experiments (we also recorded data using two perpendicular sheets, one vertical and one horizontal, both aligned in the streamwise direction). The two 0.51x0.51 m^2 samples are aligned horizontally in the same plane with a gap of 0.5 m between them. Both images are recorded simultaneously. This arrangement allows us to calculate the true spatial spectrum up to a scale of 1.5m. The process involves direct calculation of the streamwise (for example) component of the correlation tensor, $R_{ij}(r)$, whose definition is (Tennekes and Lumly, 1972):

$$R_{ij}(r) = < u_i(\vec{x},t) u_j(\vec{x}+\vec{r},t) >$$

This tensor is only a function of the separation distance, *r*, at least for homogeneous turbulence. It relationship to one dimensional spectra is

$$E_{ij}(k_1,z) = \frac{1}{2\pi}\int_{-\infty}^{\infty} R_{ij}(\Delta x)\exp(-ik_1\Delta x)d(\Delta x) \qquad E_{ij}(k_3,x) = \frac{1}{2\pi}\int_{-\infty}^{\infty} R_{ij}(\Delta z)\exp(-ik_3\Delta z)d(\Delta z)$$

where $R_{ij}(\Delta x)$ and $R_{ij}(\Delta z)$ are one-dimensional correlation functions in the streamwise and vertical directions, respectively. The two illuminated planes in Figure 1 enable us to calculate the horizontal correlation functions up to a scale of Δx_{max}=1.5 m by directly multiplying the appropriate velocity components. Up to 50 cm the two vectors are located in the same vector map and for larger scales the vectors are located in the second map. Since both images are located in the same plane with known distance between them and they are recorded at the same time, this procedure does not require any assumption of isotropy or the use of Taylor's Hypothesis. Once the correlation function is available, the energy spectrum is simply the Fourier Transform of the correlation.

The submersible system also contains the original Sea-Bird SeaCat CTD, optical transmission and dissolved oxygen content sensors, a ParoScientific Digiquartz, precision pressure transducer, a biaxial clinometer, and a digital compass. The platform is still mounted on the original hydraulic scissor-jack to enable acquisition of data at various elevations above the sea floor (the current maximum range is 1.8 m). Using a motorized drive the platform can also be rotated to align the sample area with the mean flow direction. An on-board vane that aligns itself to the flow and a video camera that focuses on this vane are used for indicating the flow direction. During the field tests we used a second submerged video camera to record images of the bottom topography.

The most recent (and by far the most successful) series of experiments took place in the vicinity of LEO 15, off the New Jersey coast in May 9-20, 2000. The exact location was 39: 27' 00" N and 74: 14' 15" W, i.e. about 0.5 nautical miles to the south-east of Node B (39: 27' 25" N, 74: 14' 45" W), and about 1.25 nautical miles to the south-east of Node A (39: 27' 41" N, 74: 15' 43" W) of LEO 15. The system was deployed from R/V Cape Henlopen (one of the UNOLS ships managed by the University of Delaware – funding for ship time was provided through NSF). The platform was deployed at a depth of 12 m and the ship was allowed to drift for a short distance before recording data. An on-board ADCP was made available and provided us with data on the mean velocity distribution in the water column for the entire duration of the tests. We also collected samples of particles at different elevations and from the bottom itself.

On the night of May 15-16 we recorded data at 0.5 Hz for eight hours continuously. On the night of May 16-17 we recorded data at 0.5 Hz for 13 hours continuously. Thus, we obtained PIV images that will enable us to study variations in flow structure and turbulence during an entire tidal cycle. The images were recorded at three different elevations, 9.5-60.5 cm, 64-115 cm and 118.5-169.5 cm above the bottom. At each elevation we aligned the system to the flow direction and then acquired data for thirty minutes, i.e. 2x1800 2Kx2K PIV images. The elevation was then changed and another image set was acquired. A sample vector map obtained during this deployment is presented in Figure 3.

On the night of May 19-20, 2000 we acquired a third data set. This time the two sample planes were perpendicular to each other and the data was acquired at 3 Hz. We recorded five data sets at different times and elevations, each consisting of 1000 image pairs. Combined, we recorded 500GB (!!) of images. Examination of numerous images, sampled randomly, reveals that the data quality, especially after enhancement (standard procedure), is exceptional with clear and dense particle traces. We are presently in the process of performing preliminary data analysis, i.e. generating vector maps of samples of data recorded in different times in order to optimize the chosen parameters for image enhancement and velocity computations (proper correlation levels, error checking, etc.). Obtaining 64x64 vectors from each image with vector spacing of 0.8 cm (the previous set provided 29x29 vectors) seems to be a straight-forward task. We are also attempting to increase the resolution to

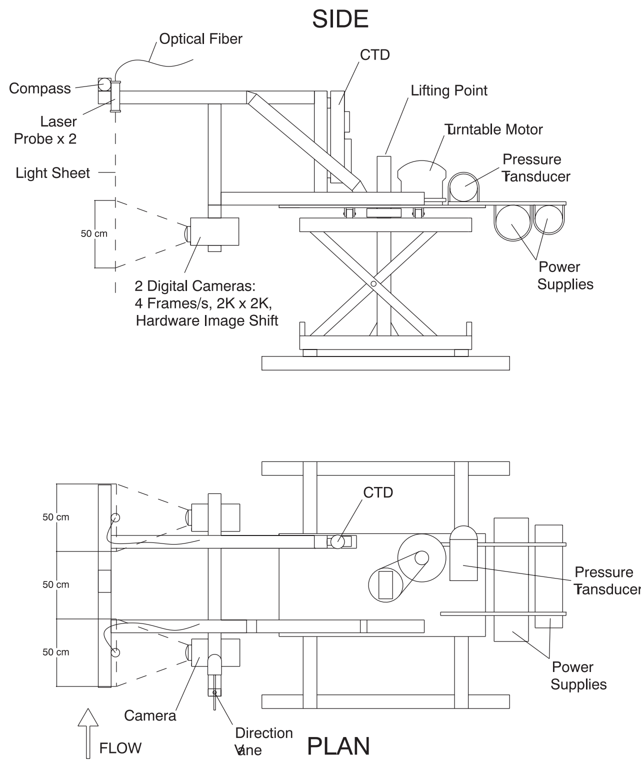

Figure 1: Two schematic views of the submersible PIV system during the deployment near LEO15, May 8-20, 2000.

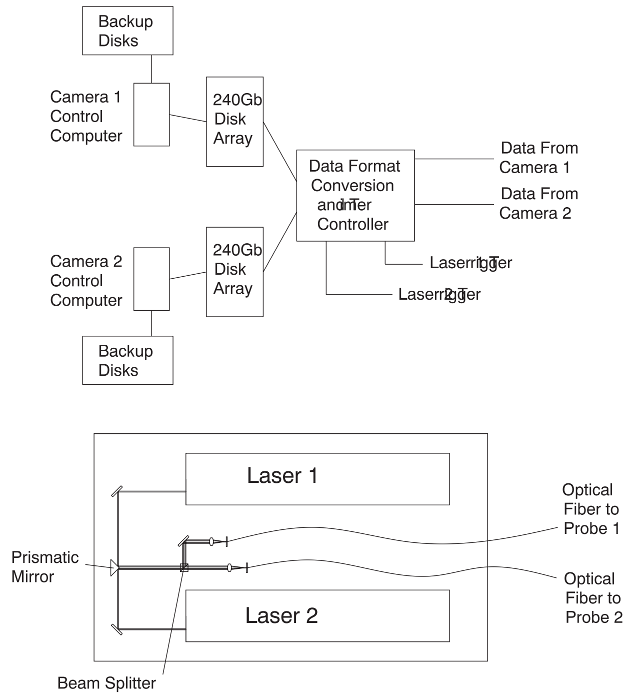

Figure 2: The surface mounted laser, control and image acquisition systems of the submersible PIV system during the recent deployments.

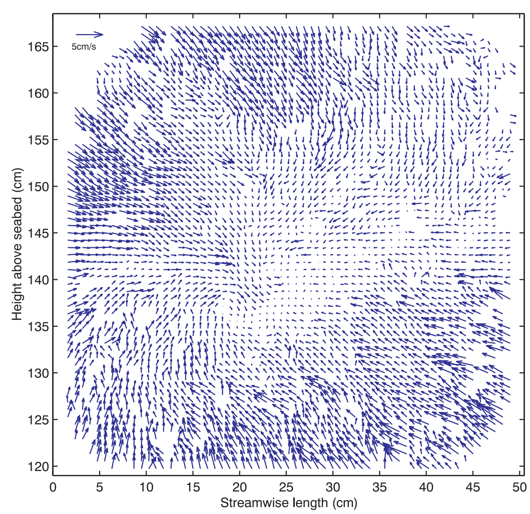

Figure 3: A sample velocity fluctuation vector map obtained during the recent deployment. Data analysis is in progress.

128x128 velocity vectors/image (vector spacing of 0.4 cm) which depends on the particle concentration. Consequently, the results will enable us to determine the true spatial spectra of the turbulence in the bottom boundary layer in wavenumbers ranging between 4.2 to 785 rad/m.

RESULTS

Currently we are processing the data obtained during the recent deployment near LEO 15. This year we have also completed the analysis of data obtained during the 1998 deployment (with the older system) and detailed results are presented in Doron et al. (2000). Some sample data has already been presented in our 1999 report. Here we would like to address the issue of turbulence anisotropy at small scales. Spatial spectra calculated from individual velocity distributions and averaged over all the realizations at the same elevation provide clear evidence that the turbulence is anisotropic at all scales including the viscous dissipation range. The vector maps are also patched together to generate extended velocity distributions using Taylor's Hypothesis. Spectra calculated from the extended data cover about three decades in wavenumber space. Unfortunately, use of Taylor's Hypothesis causes "contamination" of the data with unsteady flow due to surface waves. Nevertheless, the results still indicate that the turbulence is anisotropic also at low wavenumbers (see 1999 report).

As an illustration of the anisotropy in dissipation scales we calculate the spectral density of the instantaneous velocity from individual vector maps both in the horizontal and vertical directions. The spectra are then multiplied by k^2 and replotted to show dissipation spectra. Sample representative distributions for the six elevations of $k_1^2E_{11}(k_1)$, $k_1^2E_{33}(k_1)$, $k_3^2E_{33}(k_3)$ and $k_3^2E_{11}(k_3)$ are presented in Figure 4a-d, respectively. Clearly the data extends well beyond the peak of the dissipation spectrum. At high wavenumbers the results display a systematic peculiar phenomenon. The spectra of the velocity component parallel to the wavenumber, $k_1^2E_{11}(k_1)$ and $k_3^2E_{33}(k_3)$, have similar shapes (for five of the six cases) which are distinctly different from the spectra of the components that normal to the wavenumber, $k_1^2E_{33}(k_1)$ and $k_3^2E_{11}(k_3)$. This trend is independent of the direction relative to the mean flow. At 5 of the six elevations, the dissipation spectra of the normal velocity components have peaks at $100<k_i<250$ (Figures 4a and c), whereas in the spectra of the parallel component the dominant peaks are located in the $250< k_i <350$ range (Figure 4b and d).

In searching for plausible explanation for this phenomenon, the option of noise/error in the data is rejected since data for the same velocity component and from the same vector map are used for calculating both $k_1^2E_{11}(k_1)$ and $k_3^2E_{11}(k_3)$ and for calculating both $k_1^2E_{33}(k_1)$ and $k_3^2E_{33}(k_3)$. This trend is also not an artifact of the detrending or windowing procedures, since it is observed even when no windowing or detrending is applied. At this stage we do not have an explanation for this trend.

The only exception is the data for $96<z<116$ cm, the last data set recorded. For this case the dissipation spectra have substantially higher magnitudes and both parallel and normal components have peaks at $250< k_i <350$. The mean velocity at this elevation (Doron et al., 2000) is also higher. Since the measurements at different heights are performed at different times (with 15 minutes interval), it is possible that the difference between this elevation and the others is caused by changes in the flow conditions at the time that the measurements take place. Using "Tides and Currents v.2" (Nautical Software, Inc.) to estimate the variations of the tidal current at the nearest locations we obtain that this last measurement was performed shortly after the tide reversed direction.

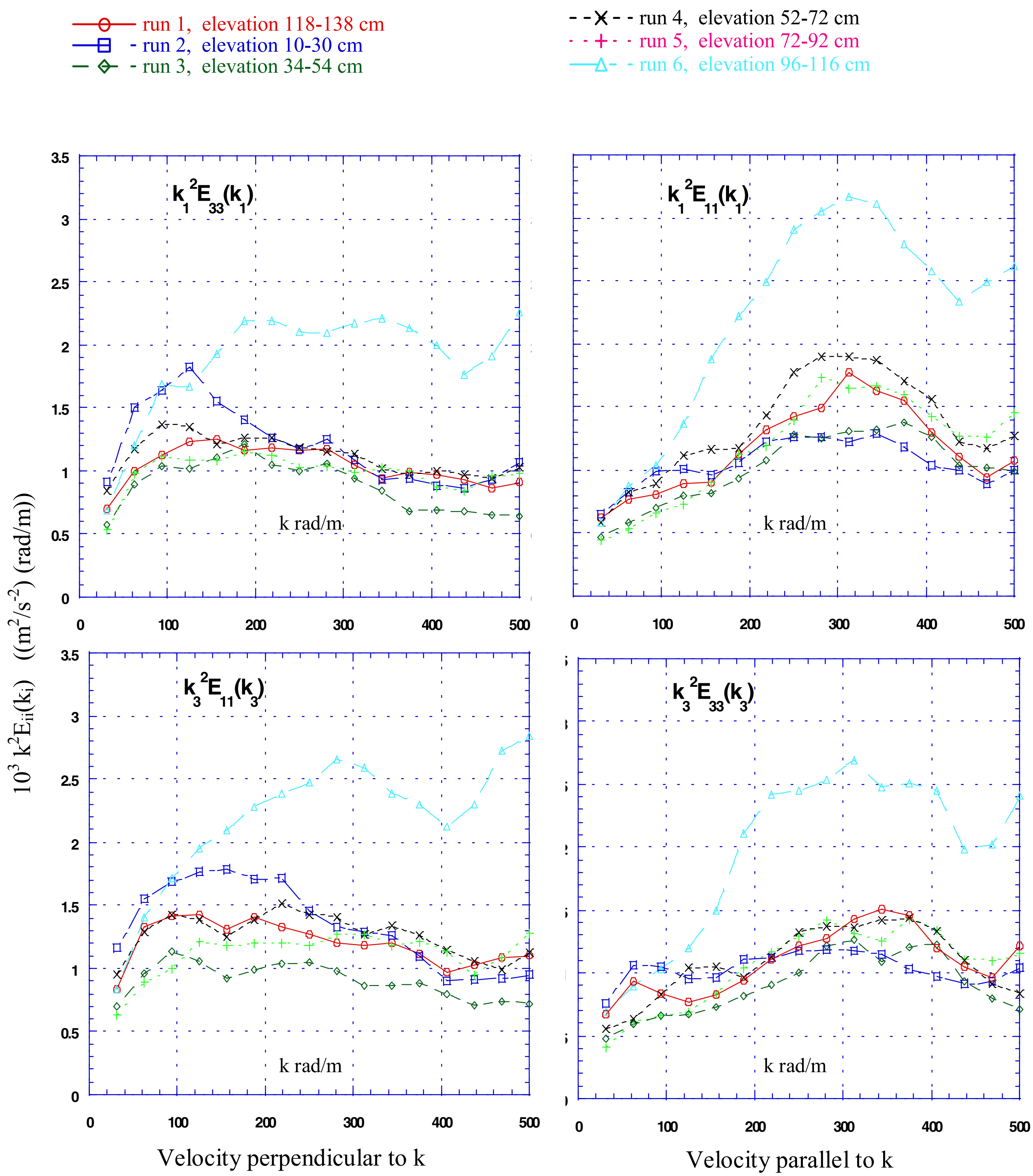

Figure 4: Spatial dissipation spectra at different elevations. Each line is an average of 3 rows (or columns) and 130 vector maps.

IMPACT/APPLICATIONS

The present measurements provide us with a unique opportunity to address a series of issues related to flow structure and turbulence in the bottom boundary layer of the coastal ocean. Included are distributions of Reynolds shear stresses, energy and dissipation spectra as well as turbulence production and dissipation, all free of contamination by surface waves. We can also determine the effects of large scale forcing on these parameters, study the dynamics of large-scale turbulent structures and their effect on sediment entrainment, and address fundamental questions related to applications of Large Eddy Simulations (LES) to oceanic flow modeling.

TRANSITIONS

During FY 2000 the submersible PIV system described in this report has been used extensively at NSWC/Carderock to measure the flow structure within wakes behind maneuvering submerged models.

REFERENCES

Bertuccioli, L., Roth, G.I., Katz, J., and T.R. Osborn, 1999: Turbulence measurements in the bottom boundary layer using particle image velocimetry. *Journal of Atmospheric and Oceanic Technology.* **16**, 1635-1646.

Tennekes, H., and J.L. Lumley, 1972: *A First Course in Turbulence*, MIT Press, Cambridge, MA.

PUBLICATIONS

Doron, P., L. Bertuccioli, J. Katz, and T.R. Osborn, 2000: Turbulence Characteristics and Dissipation Estimates in the Coastal Ocean Bottom Boundary Layer from PIV Data. Accepted for publication in the *Journal of Physical Oceanography*.

Bertuccioli, L., Doron, P., Katz, J., Osborn, T., (2000), “PIV Measurements Of turbulence Characteristics and Dissipation in The Bottom Boundary layer of The Coastal Ocean,” ASLO - AGU Ocean Science Meeting, San Antonio, TX, January 24-28, in EOS Transactions, Vol. 80, No. 49, p. OS 120, December, 1999.